Atomistic Study of Sulfur Diffusion and S2 Formation in Silicon during Low-temperature Rapid Thermal Annealing

Takahisa Kanemura, Koichi Kato*, Hiroyoshi Tanimoto, Nobutoshi Aoki, and Yoshiaki Toyoshima
Center for Semiconductor Research and Development, Semiconductor & Storage Products Company, Toshiba Corporation,
*Advanced LSI Technology Laboratory, Corporate Research and Development Center, Toshiba Corporation,
Kawasaki, Japan.

***Abstract*— Theoretical analyses predict that large Schottky barrier reduction by sulfur doping at NiSi/Si junction is induced by S2 formation. The S2 formation may have occurred in silicidation process, even under low temperature rapid thermal annealing. We have demonstrated that implanted sulfur into silicon forms S2 configuration under low temperature rapid thermal annealing, based on first principles calculations and kinetic Monte Carlo (KMC) simulations.**

Keywords—Kinetic Monte Carlo Simulations; First Principles Calculations; Sulfur; Silicon;Diffusion

I. INTRODUCTION

Sulfur doping at NiSi/Si junction has been found to make a Schottky barrier height ultimately small, revealing almost zero junction resistance [1-2]. Theoretical analyses predict that the large barrier reduction is induced by S atom pair (S2) in the vicinity of NiSi/Si junction [3]. The S2 formation in a crystalline Si has been experimentally suggested by infrared absorption and photoconductivity spectra. The sample in their work was annealed with a long time (8-260h) and a high temperature (825-1100 °C) [4]. Low-temperature (400-700 °C) and short-time (order of seconds) anneal is, however, generally indispensable for silicidation process. It is, therefore, important to study the behavior of sulfur atoms in Si during low-temperature rapid thermal annealing (LT-RTA). In this paper, we examine whether S2 formation actually occurs or not in LT-RTA by combining first principles calculations and kinetic Monte Carlo (KMC) simulations.

II. MODEL

To simulate dynamics of sulfur during implant and LT-RTA, we considered six atomic configurations of sulfur in Si (Fig. 1). The binding energies of these configurations, being obtained by first principles calculations [5], are listed in Fig. 1. This "binding energy" was an energy gain of the system upon formation of stable complexes from well-separated elemental defects, that is, silicon self-interstitials (I), vacancies (V) and substitutional sulfur atoms (S_{sub}). Configurations with larger binding energy are energetically more stable. We assumed that a sulfur atom at an interstitial site (S_{int}) has lowest migration energy among sulfur configurations, because sulfur diffusion is observed as silicon self-interstitial assisted mechanism [6]. The S_{int} migration energy by first principles calculations was 1.8 eV, being agreed with the experimental value [7]. Sulfur atoms of S2 occupy nearest-neighbor substitutional sites. The pair has no covalent bond to each other, and an electronic charge at donor level for each atom as shown in Fig. 2. In SV, SV_2 and S2V, sulfur atoms and vacancies were located at lattice sites. We also calculated energy of three types of sulfur configurations on Si/SiO_2 interface, where the sulfur was

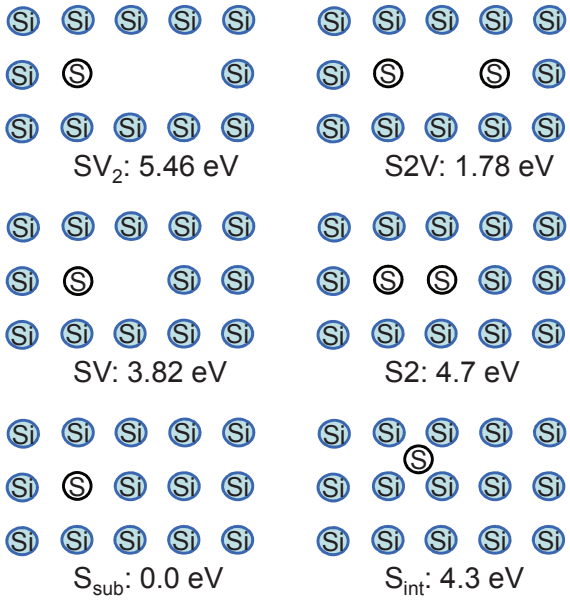

Fig. 1. Schematic configurations of S-defect complexes in the KMC simulations and their binding energies obtained by the first principles calculations.

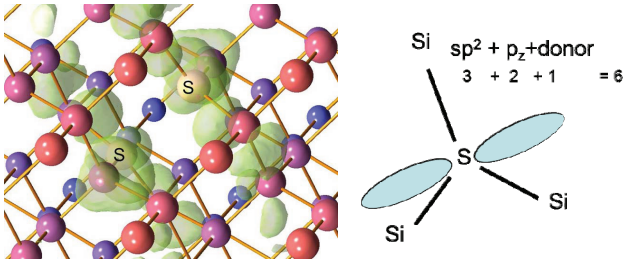

Fig. 2. (Left side) Atomic geometry and electronic configurations of an S2 in a bulk Si, using first principles calculations. Balls with no atomic symbol represent Si atom. (Right side) Schematic "sp^2 + pz + donor" configuration formed by 6 valence electrons of each sulfur atom.

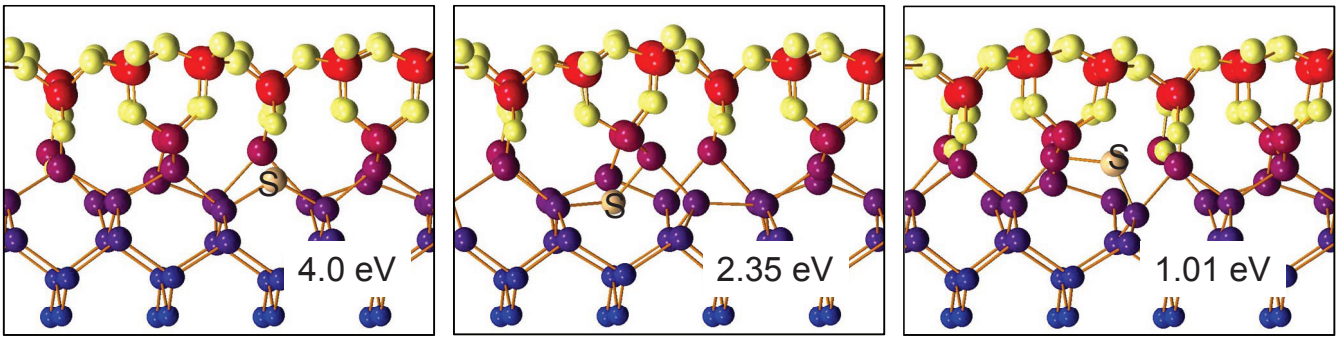

Fig. 3. Atomic geometries of sulfur captured at a vacancy site at SiO_2/Si interface (left), a neighbor site of the vacancy (center) and a perfect interface (right), and their binding energies between S_{int} and capture sites. Yellow balls with no atomic symbol represent O atoms and red, blue and violet balls represent Si.

captured at a silicon vacancy site at the interface, at a neighbor site of the vacancy, and at a perfect interface. These configurations and the binding energies between S_{int} atoms and capture sites are shown in Fig. 3. The interface defect, which is the vacancy of capturing site for S_{int}, is found to be most stable configuration.

Using in-house non-lattice KMC simulator, similar to DADOS [6], we simulated migrations of I, V and S_{int}, captures by and emissions from defects including these complexes. The captures and emissions concerning sulfur complexes are forward and reverse reactions of followings, respectively.

$$S_{int} + S_mV_n \leftrightarrow S_{m+1}V_{n-1} \quad (1)$$

$$I + S_mV_n \leftrightarrow S_mV_{n-1} \quad (2)$$

$$V + S_mV_n \leftrightarrow S_mV_{n+1} \quad (3)$$

$$S_{int} + S_mV_n \leftrightarrow S_{sub} + S_mV_{n-1} \quad (4)$$

$$S_{int} + S_mV_n \leftrightarrow I + S_{m+1}V_{n-1} \quad (5)$$

$$S_{int} + I_mV_n \rightarrow S + I_{m+1}V_n \quad (6)$$

$$S_{int} + I_m \leftrightarrow S + I_{m+1} \quad (7)$$

$$S_{int} + V_m \rightarrow S + V_{m-1} \quad (8)$$

Here, m and n are zero or positive integers. S_1V_0 and S_1I_1 are equivalent to S_{sub} and S_{int}, respectively. I_mV_n for $m \geq 1$ and $n \geq 1$ in (6) is an implant-induced defect "amorphous pocket", introduced in DADOS. In reactions (4)-(8), only I or S component of S_{int} is captured. The captures are controlled by diffusions of mobile species (I, V, S_{int}). In the case of endothermic reaction, the capture probabilities decrease exponentially, when the activation energies increase. The activation energies E_a of the reactions, with the heat of the reactions ΔH and emitting the species which has the migration energy E_{mig}, are assumed as following.

$$E_a = \max(E_{mig} + \Delta H, 0) \quad (9)$$

A jump length per one migration or one emission in KMC simulations was set to 0.384nm. A pre-exponential factor of S_{int} migration frequency was determined by the experimental diffusion coefficient of sulfur [7]. And pre-exponential factors of emissions were determined so as to reproduce experimental results of sulfur diffusion in Si [1], as shown in Fig. 4. This figure implies reasonable agreement between simulation results and experimental ones.

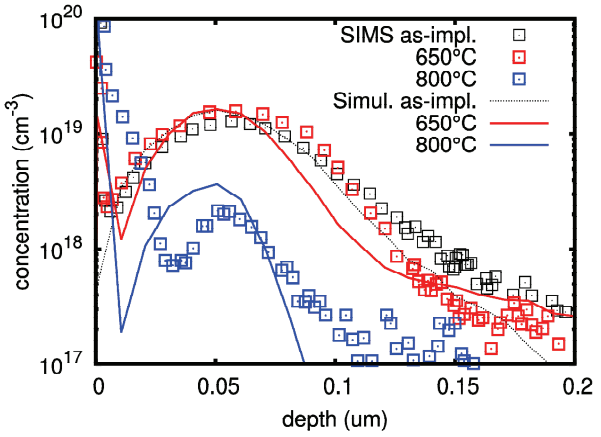

Fig. 4. SIMS and simulated profiles of sulfur after 50 keV 1e14 cm^{-2} S implant and subsequent RTA at 650 and 800 °C for 1 minute.

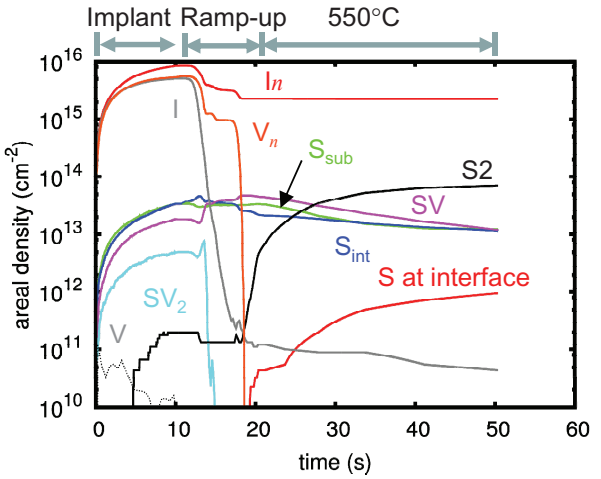

Fig. 5. Time evolution of areal density of various silicon self-interstitial, vacancy and sulfur complexes during implant and subsequent 550 °C RTA.

III. RESULT

We performed KMC simulation for 50 keV 1e14 cm^{-2} S implant and subsequent RTA. Temperature of RTA was varied from 550 °C to 800 °C, and the anneal time was varied from 3 s to 18 min. We chose 550 °C and 30 s, being the typical process conditions for silicidation [1]. We assumed that the temperature and time for implant were 30 °C and 12 s respectively, and the temperature ramp-up rate in RTA was 50 °C/s.

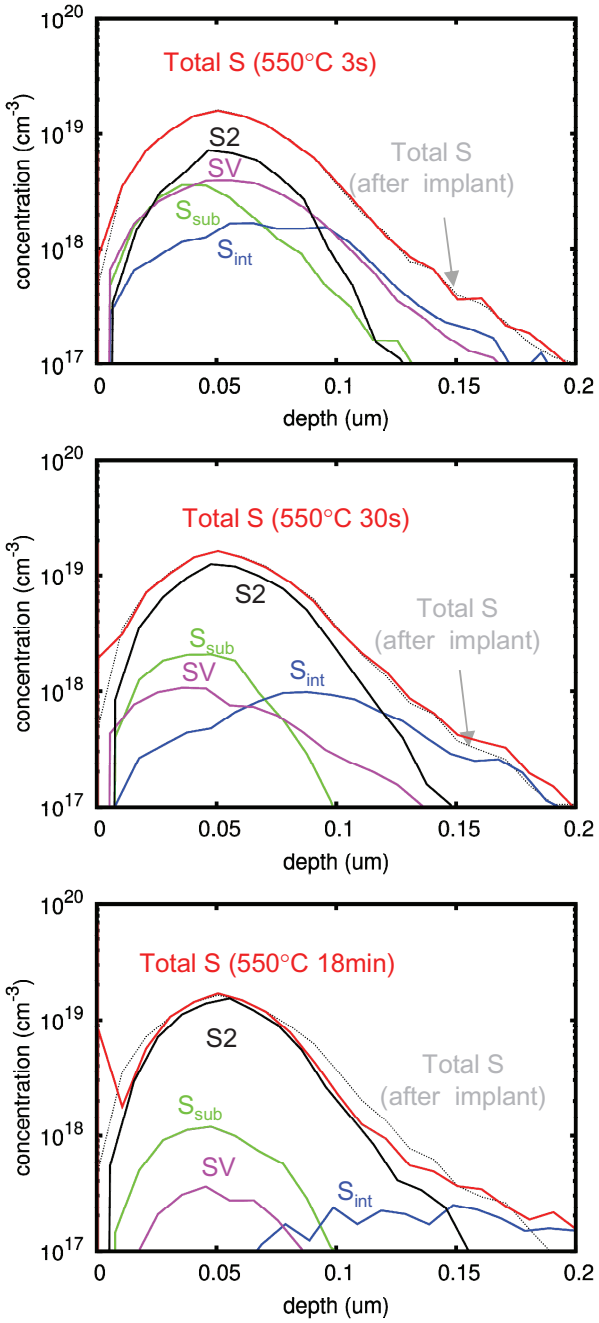

Fig. 6. Simulated profiles of sulfur in various sulfur complexes after implant and subsequent RTA at 550 °C for 3 s.(top), 30s.(middle) and 18min (bottom).

Figure 5 shows the time evolution of areal densities of various silicon self-interstitial, vacancy and sulfur configurations in 1e14cm^{-2} dose and 550 °C. At the end of the implant, S2 density was very low, because S_{int} migration and collision to other sulfur atom rarely occur at room temperature. Most of sulfur atoms formed S_{int} and S_{sub}. During ramp-up period, vacancy clusters were dissolved completely, releasing vacancies. The vacancy migrated very frequently, and vanished at interface or collided to S_{sub}. Consequently reaction $V + S_{sub} \rightarrow SV + 3.67eV$ occurred and SV increased. From the end of ramp-up and during the holding time at temperature 550 °C, S2 increased while S_{int}, S_{sub}, and SV decreased. These are enhanced by the reaction $S_{int} + S_{sub} \rightarrow I + S2 + 0.48eV$ and by the reaction $S_{int} + SV \rightarrow S2 + 4.10eV$. These reactions are triggered by slow migrating S_{int}. We also see that sulfur atoms were captured at interfaces gradually. Consequently, the depth profile of the most stable S2 after 3 s, 30 s and 18 min RTA does not change much, as shown in Fig. 6. A peak of S2 profile is located at almost the same peak of implanted profile. S_{int} profile became broader as time progressed.

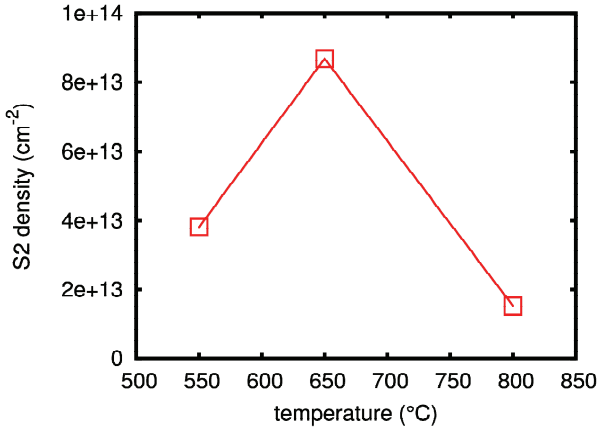

Fig. 7. RTA temperature dependence of S2 density. RTA time were 30 s.

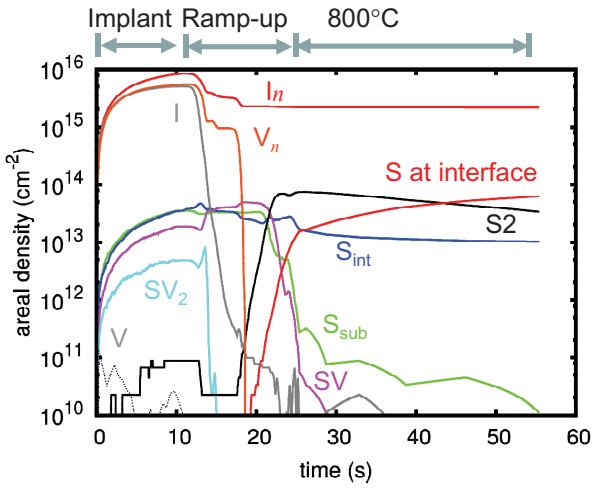

Fig. 8. Simulated profiles of sulfur in various silicon self-interstitial, vacancy and sulfur complexes after implant and subsequent RTA at 800 °C for 30 s.

Figure 7 shows the RTA temperature dependence of S2 density after 1e14cm^{-2} implant. S2 density at 650 °C is higher than at 550°C because S2 formation reaction proceeds faster with highly activated S_{int} migration at 650 °C. On the other hand, S2 density at 800 °C is lower than at 650°C because the S2 formation reaction is suppressed. Figure 8 shows time evolution of sulfur configuration in 800 °C RTA. Compared to the case of 650 °C, the reaction $S_{sub} \rightarrow S_{int} + V$ -3.08eV frequently occurred rather than the S2 formation reaction $S_{int} + S_{sub} \rightarrow I + S2 + 0.48eV$. Therefore the S_{sub} density became lower and S2 formation was suppressed. As time progress, S2 decreased through the reaction $I + S2 \rightarrow S_{int} + S_{sub}$ - 0.48eV.

IV. CONCLUSION

We demonstrated that S2 formation in Si really occurs by 50 keV 1e14 cm^{-2} S implant and subsequent RTA at 550 °C. The S2 formation reactions were $S_{int} + S_{sub} \rightarrow I + S2 + 0.48$ eV and $S_{int} + SV \rightarrow S2 + 4.10$ eV. These reactions are triggered by slow migrating $S_{int.}$ This is consistent with the ultimate low Schottky barrier due to sulfur doping and LT-RTA [2]. S2 formation reaction is more enhanced with highly activated S_{int} migration by increasing the temperature up to 650 °C. As the temperature is increased up to 800 °C, the formation reaction $S_{int} + S_{sub} \rightarrow I + S2 + 0.48$ eV is suppressed because the reaction $S_{sub} \rightarrow S_{int} + V$ -3.08eV is activated. The produced S2 is dissolved by the reaction $I + S2 \rightarrow S_{int} + S_{sub}$ - 0.48 eV.

REFERENCES

[1] Q. T. Zhao, U. Breuer, St. Lenk, and S. Mantl, "Segregation of ion implanted sulfur in Si(100) after annealing and nickel silicidation," J. Appl. Phys., vol. 102, p. 23522, 2007.

[2] Y. Nishi and A. Kinoshita, "NiSi metal S/D transistors with ultimately low Schottky barrier by sulfur implantation after silicidation process," Extended Abstracts of the 2009 International Conference on Solid State Devices and Materials, pp. 771-772, 2009.

[3] K. Kato, Y. Nishi, and Y. Mitani, "The electronic structure of an S-pair in barrier-less metal/silicon junctions," ICPS 2012 - 31st International Conference on the Physics of Smiconductors, 37.37, 2012.

[4] E. Janzen, R. Stedman, G. Grossmann, and H. G. Grimmeiss, "High-resolution studies of sulfur- and selenium-related donor centers in silicon," Phys. Rev. B, vol 29, p. 1907, 1984.

[5] K. Kato, "Gate bias polarity dependent H migration and O vacancy generation through Si=O–H complex formation in SiO_2/Si(100)," Phys. Rev. B, vol 85, p. 85307, 2012.

[6] N. A. Stolwijk, D. Grunebaum, M. Perret, and M. Brohl, "Zinc and Sulphur in Silicon, Experimental Evidence for Kick-Out Diffusion bihaviour," Mater. Sci. Forum, vol. 38-41, pp. 701-706, 1989.

[7] F. Rollert, N. A. Stolwijk, and H. Mehrer, "Diffusion of sulfur-35 into silicon using an elemental vapor source," Appl. Phys. Lett., Vol. 63, pp. 506-508, 1993.

[8] M. Jaraiz, M., L. Pelaz, L., E. Rubio, J. Barbolla, G. H. Gilmer, D. J. Eaglesham, ... , and J. M. Poate, "Atomistic modeling of point and extended defects in crystalline materials," MRS Proceedings Vol. 532, No. 1. Cambridge University Press, 1998.